Japanese Journal of Applied Physics

The Japan Society of Applied Physics

REGULAR PAPER

Plasma assisted-MBE of GaN and AlN on graphene buffer layers

To cite this article: D. P. Borisenko *et al* 2019 *Jpn. J. Appl. Phys.* **58** SC1046

View the article online for updates and enhancements.

This content was downloaded from IP address 46.216.181.51 on 27/01/2020 at 11:23

Japanese Journal of Applied Physics 58, SC1046 (2019)
https://doi.org/10.7567/1347-4065/ab124b

REGULAR PAPER

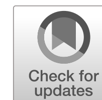

Plasma assisted-MBE of GaN and AlN on graphene buffer layers

D. P. Borisenko[1*], A. S. Gusev[1*], N. I. Kargin[1], I. V. Komissarov[1,2], N. G. Kovalchuk[2], and V. A. Labunov[1,2]

[1]National Research Nuclear University MEPhI, Moscow, 115409, Russia
[2]Belarusian State University of Informatics and Radioelectronics, Minsk, 220013, Belarus

*E-mail: DPBorisenko@mephi.ru; ASGusev@mephi.ru

Received December 14, 2018; accepted March 13, 2019; published online May 22, 2019

The possibility of using chemical vapor deposition (CVD) graphene as a 2D buffer layer for epitaxial growth of III-nitrides by plasma assisted-MBE on amorphous substrates (SiO_2 prepared by thermal oxidation of Si wafer) was investigated. The comparative study of graphene-coated parts of the wafers and the parts without graphene was carried out by scanning electron microscopy and X-ray diffractometry. It was shown that epitaxial GaN and AlN films with close to 2D surface morphology can be obtained by plasma assisted-MBE on amorphous SiO_2 substrates with a multilayer graphene buffer using the HT AlN nucleation layer. © 2019 The Japan Society of Applied Physics

1. Introduction

III-nitride semiconductors and their alloys have attracted considerable attention because of their outstanding properties leading to many applications for light-emitting diodes, laser diodes, high-frequency and high-power transistors.[1–4)] Absolute majority of the GaN-based devices are fabricated on single-crystal sapphire and 4H- or 6H-SiC substrates because native substrates are not available at high quality and sufficient sizes. The main drawback of these commercial substrates—the high cost. In contrast, silicon (111) substrates are large in area (up to 8 inches) and inexpensive. The price per unit area of Si wafer is about 1/10 of that of a sapphire and about 1/100 of that of a SiC substrate.[5)] Silicon has relatively high thermal conductivity (compared to sapphire) and it can be easily removed after $A^{III}N$ growth procedure. However, the epitaxial growth of III-nitrides on Si is challenging because of highly different materials properties. There is a considerable lattice mismatch (18%) and large thermal expansion coefficient mismatch (46%) between GaN and Si.[6)] Such a lattice and thermal mismatch can lead to high stresses and bowed wafers. Moreover, the high initial dislocation density caused by the lattice mismatch needs to be reduced.

Since graphene has a hexagonal lattice with low lateral mismatch, it can be considered as a 2D buffer layer for wurtzite GaN and AlN epitaxy[7–15)] on silicon or even amorphous substrates. The first studies[7–9)] in this direction were devoted to GaN growth on ZnO coated graphene layers by metal-organic chemical vapor deposition (MOCVD) method. Then attempts were made to grow gallium nitride by the method of plasma assisted molecular beam epitaxy (PA-MBE)[11)] on the single layer CVD graphene transferred directly to the surface of Si (100) wafer. However, the GaN epitaxial layers obtained on both 1 ML graphene coated and pure silicon showed a pronounced columnar morphology with a grain size in the range of 0.1–1 μm.[11)] It was later shown that the GaN epitaxial films with improved crystal quality and good morphology can be obtained by pulsed sputtering[10)] or MOCVD[12–14)] on the surface of multilayer graphene. Therefore, the purpose of this work was to investigate the possibility of CVD multilayer graphene using as a buffer layer for epitaxial growth of III-nitrides (GaN and AlN) by PA-MBE on amorphous substrates (SiO_2 layers prepared by thermal oxidation of Si wafers) that unlike the pure Si(100)[11)] or Al_2O_3[14)] surface do not have any epitaxial relationships with GaN (or AlN). It should be noted that such structures (like ≪GaN-on-Si≫) may be of interest when developing new devices based on $A^{III}N$ heterostructures in combination with conventional silicon CMOS technology.

2. Experimental methods

In this paper, the multilayer graphene films were grown by chemical vapor deposition (CVD) on 60 μm thick copper foil (99.9% purity, as evidenced by the EDX study) using n-decane ($C_{10}H_{22}$) as a carbon source[16)] and then transferred onto the surface of 2-inch Si wafers with 300 nm thick thermal oxide. The root mean square roughness (RMS) for the oxide surface calculated from AFM data [Fig. 1(a)] was around 0.3 nm.

Prior to the CVD growth, the Cu foil was electrochemically polished for 5 min in 1 M phosphoric acid at a bias voltage of 2.3 V. A custom-made CVD set-up with a 14 mm diameter tubular quartz reactor was employed for the experiment. The 35×45 mm^2 sample was placed in the middle of the reactor. One side of the copper foil covered the inner wall of the quartz tube. Then the catalyst was annealed for 1 h at 1050 °C in the presence of N_2 and H_2 gas flow at a rate of 100 and 150 cm^3 min^{-1}, respectively. The purity of the nitrogen gas was 99.95% and the purity of the hydrogen was 99.99%. After that the n-decane was introduced into the tubular quartz reactor for 30 min (at 1050 °C). Due to the fact that n-decane is a colorless volatile liquid with a flash point of about 46 °C, it was introduced into the reactor via bubbler system (evaporator for liquid precursor). The bubbler system contains the thermostat part where the temperature is stabilized by iced water. Argon was passed through the bubbler as a carrier gas (≈200 cm^3 min^{-1}). At the same time the feeding rate of n-decane was estimated to be 4 μl min^{-1}. At the end of the process the quartz reactor was cooled down at a rate of 50 °C min^{-1} in the presence of N_2 gas flow.

The transfer of graphene from the original to the arbitrary substrate without deteriorating the crystallinity of the graphene is still a challenging task. In this work, we employed a wet-chemical room temperature transfer process onto SiO_2/Si substrates without the use of a polymer support. The copper foil was totally dissolved in a water solution of $FeCl_3$. The graphene film was gently washed several times in a bath with distilled water prior to the transfer onto the target substrate [Fig. 1(b)]. The RMS parameter has not changed

© 2019 The Japan Society of Applied Physics

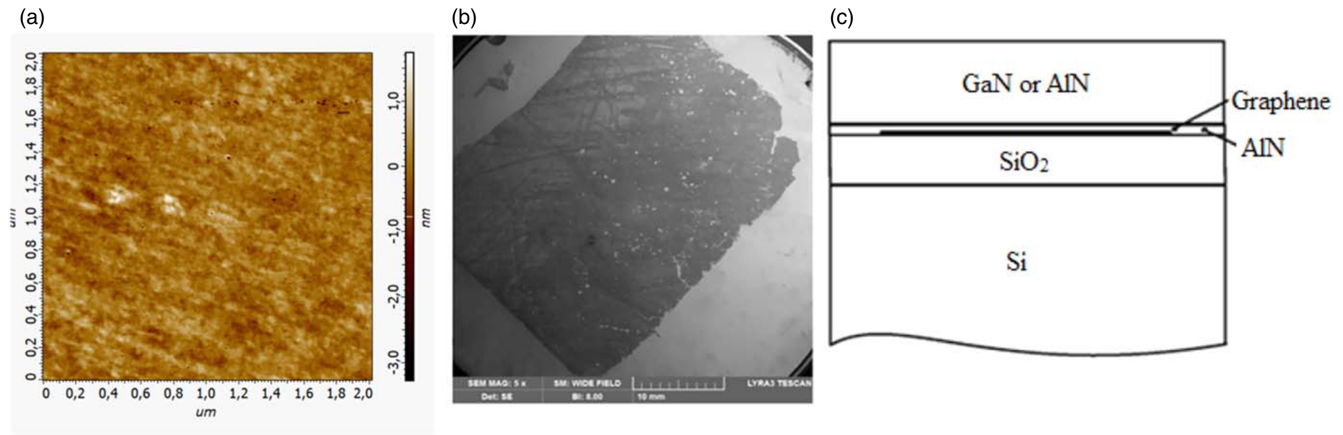

Fig. 1. (Color online) Atomic force microscopy height image for the oxide surface (a); the low-zoom SEM image of the graphene layer on the surface of 2-inch Si wafer (with thermal oxide film) before the MBE growth process (b); cross section scheme of the experimental structure (c).

and amounted to 0.3 nm in defect free sites. After the transfer, multilayer graphene is characterized by a continuous film with a low number of breaks, cracks and folds, which is in good agreement with the results of atomic force microscopy.

The graphene samples obtained under the above listed conditions were analyzed by Raman spectroscopy using the Confotec NR500 confocal micro-Raman spectrometer with 473 nm excitation wavelength. A 3D scanning laser confocal micro-Raman spectrometer (Confotec NR500) allowed for the acquisition of two kinds of images within a single scan: a Rayleigh image, using laser light reflected from a sample, and a spectral image by Raman scattering. The spectral resolution was about 3 cm^{-1}. We also proved homogeneity directly by the light transmittance measurement of samples transferred on a glass substrate. The diameter of probed area was 0.5 cm. The transmittance at 550 nm was 94%. This value corresponds to a number of graphene layers between 2 (95.5%) and 3 (93.3%). This is in good agreement with the micro-Raman findings (the number of graphene layers was estimated from the lines intensities ratio I(2D)/I(G)). The Raman integral intensity ratio ID/IG provides information about the concentration of point defects n. From the experimental results we get $n \approx 2.2 \times 10^{11}$ cm^{-2}. These experimental procedures and results were previously described by us in detail.[16,17]

GaN and AlN epilayers were grown by PA-MBE using Veeco GEN 930 setup equipped with a UNI-Bulb Veeco RF nitrogen plasma activator. The RF plasma power and nitrogen flow rate were 350 W and 1.6 sccm, respectively. The background pressure in the growth chamber was 1×10^{-10} Torr. First, a substrate was annealed in vacuum at a temperature of 710 °C for half an hour. The growth of both AlN and GaN layers was started with a high temperature (HT) nucleation of a 20–30 nm-thick AlN layer at $T_s = 710$ °C under nitrogen-rich mode ($F_{Al}/F_N \approx 0.6$). After that a 500 nm thick layer of GaN (or 300-nm-thick AlN) was grown under metal-rich conditions ($F_{Me}/F_N > 1.5$) at the same substrate temperature [Fig. 1(c)]. The pressure during growth was $\approx 1 \times 10^{-5}$ Torr. The formation of the metal microdroplets under these conditions was avoided by using Ga (or Al) flux interruptions with duration controlled by pyrometry.[18,19] The nucleation and growth were also monitored in situ by reflection high-energy electron diffraction technique (RHEED).

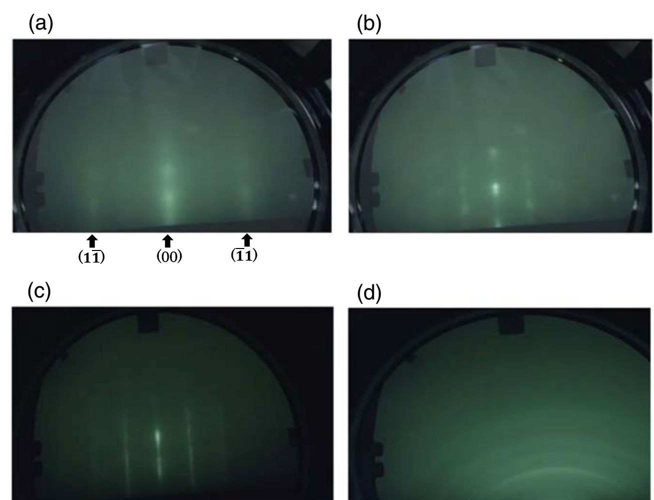

Fig. 2. (Color online) RHEED patterns obtained from the multilayer graphene prior to the MBE growth (a), during the nucleation process (b) and during the long-term MBE GaN growth (c) on graphene coated part of the wafer. RHEED pattern for the part of the same wafer without graphene buffer (d) during the long-term MBE growth is given for a comparison.

In the final step, the comparative study of graphene-coated parts of the wafers and the parts without graphene was carried out by scanning electron microscopy (SEM; LYRA 3, Tescan) and high-resolution X-ray diffractometry (XRD) including XRD pole figures method. XRD patterns of the experimental samples were collected using CuK_α ($\lambda = 0.15406$ nm) radiation with Ultima IV (Rigaku) diffractometer in $2\theta/\omega$ geometry.

3. Results and discussion

RHEED patterns prior to the growth process, during the nucleation and following growth stages were monitored using a 15 kV RHEED system including CCD camera and a commercial software. Figure 2(a) shows the RHEED pattern from the multilayer graphene transferred to a SiO_2/Si substrate. Here the central streak represents the (00) lattice of the reciprocal space of graphene, while additional side streaks come from (1$\bar{1}$) and ($\bar{1}$1) Bragg reflection.[20,21] The spread of the streaks is probably due to the electron scattering from the graphene wrinkles which are always exist in the real system. The next RHEED pattern [Fig. 2(b)] demonstrates the heterogeneous nucleation of AlN and islands coalescence

© 2019 The Japan Society of Applied Physics

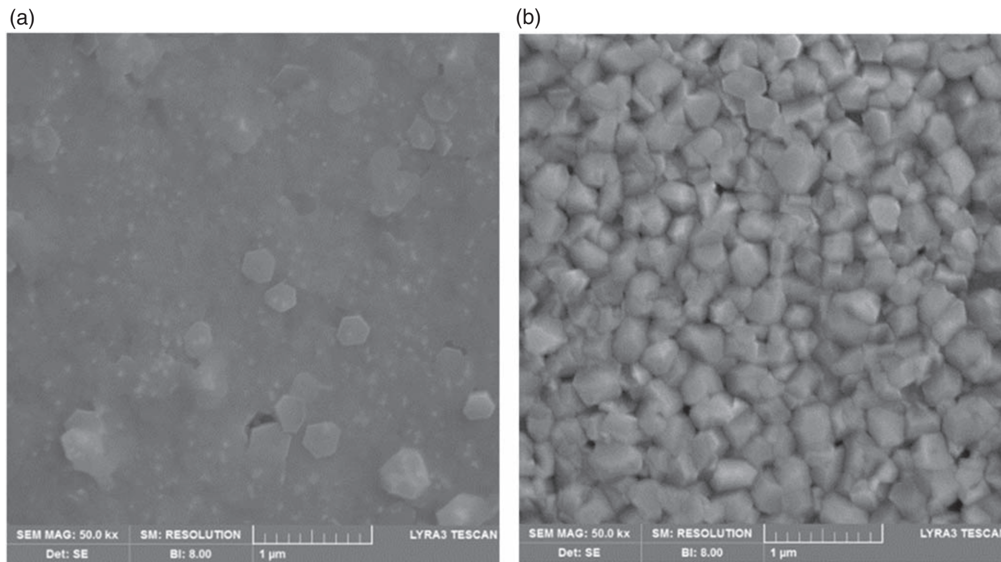

Fig. 3. SEM images: (a) the surface of GaN film on the graphene coated part of the substrate, (b) the surface of the GaN film on SiO_2.

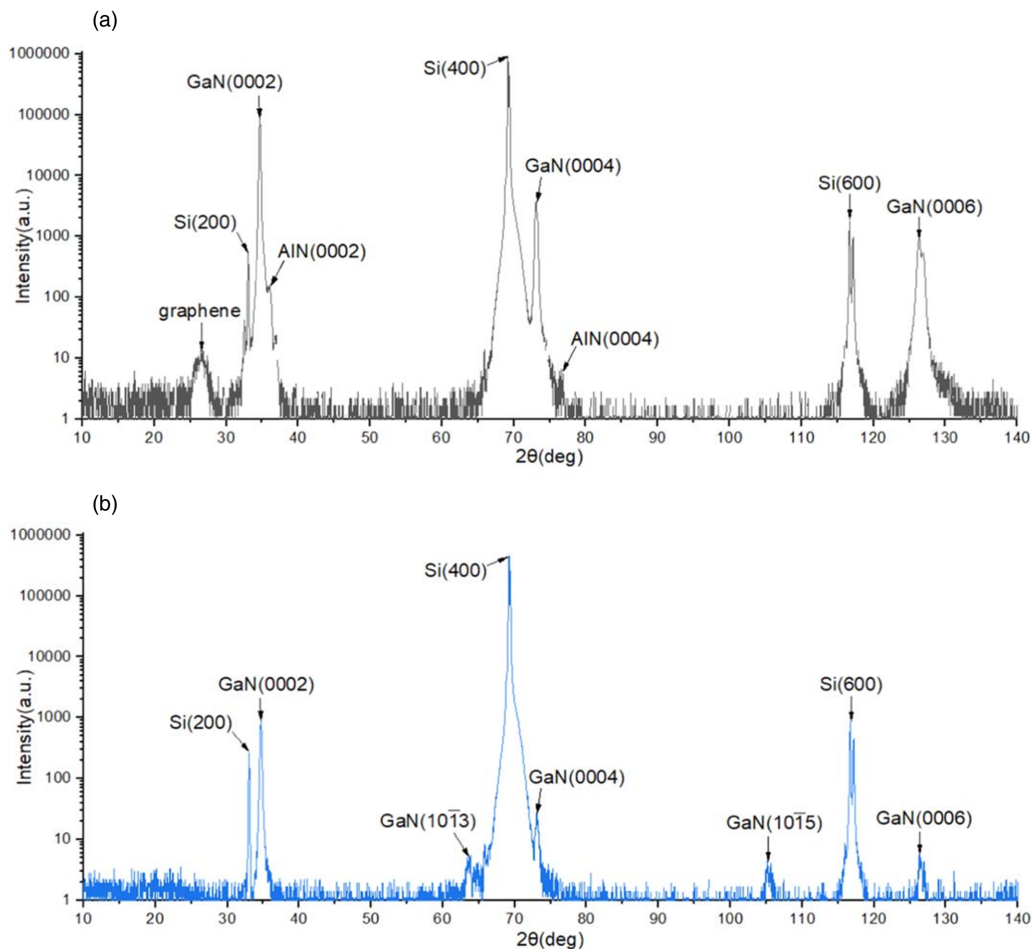

Fig. 4. (Color online) X-ray diffraction spectra of GaN film grown on the graphene coated part (a) and the SiO_2 part (b) of the same wafer.

process at the first stage of MBE growth on the graphene coated part of the SiO_2 substrate. Shown in Fig. 2(c) is the RHEED pattern of the GaN film in the $\langle 11\bar{2}0 \rangle$ azimuth direction during the long-term epitaxy under the above listed conditions. Such well-developed streaky 1×1 RHEED pattern was formed after approximately 200–300 nm thick GaN layer deposition under the Ga-rich regime. It contains elongated streaks with intensity modulation in the perpendicular direction indicating presence of multilevel terraces of different widths on the growth surface.[22] This 1×1 RHEED pattern transforms to the 2×2 surface structure gradually when the Ga shutter is closed which allows talking about the $\ll$Ga$\gg$ polarity of the experimental sample.[23] At the same time the RHEED image changed to a ring pattern [Fig. 2(d)]

© 2019 The Japan Society of Applied Physics

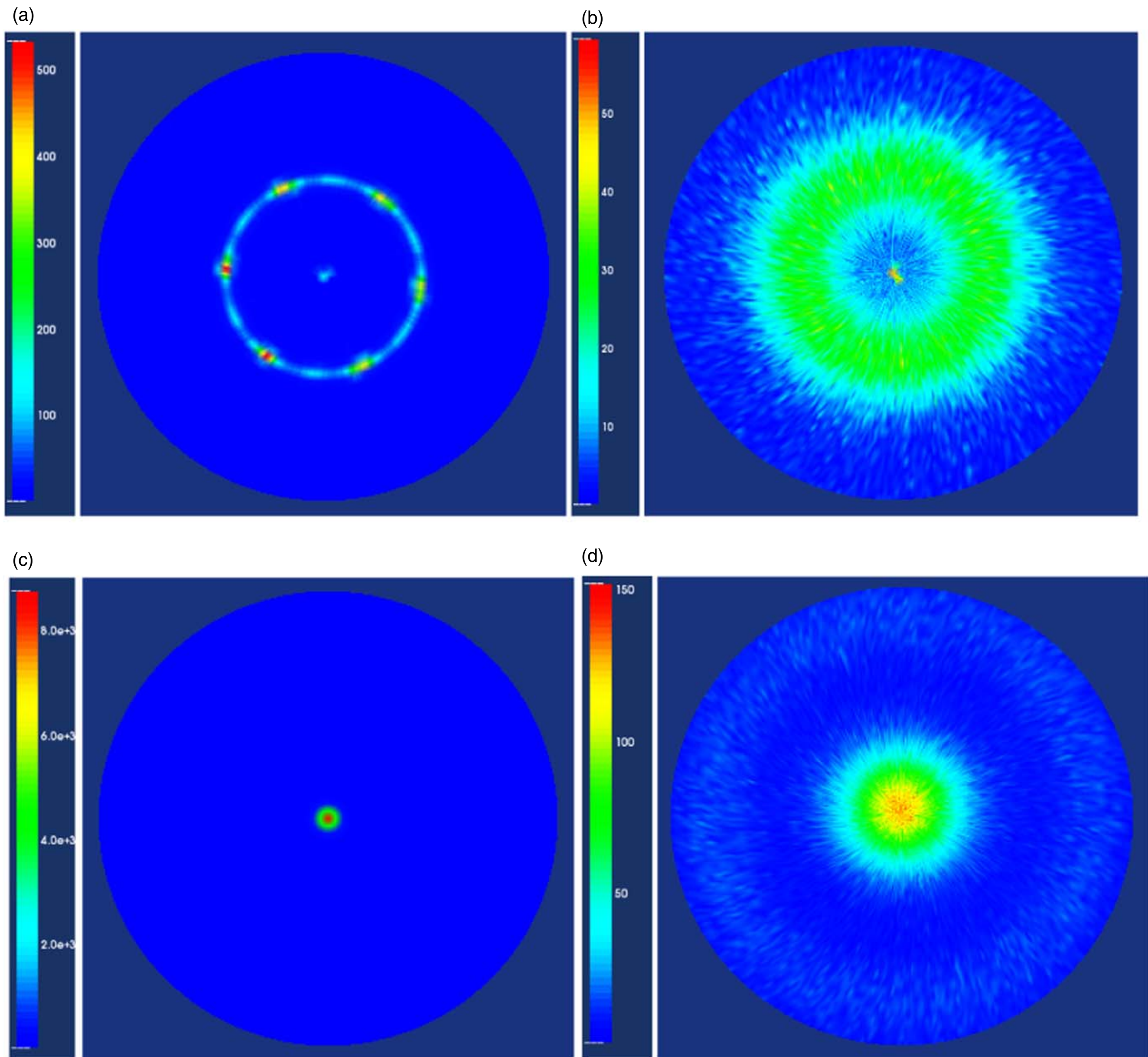

Fig. 5. (Color online) XRD pole figures for the GaN $\{10\bar{1}3\}$ ($2\theta = 63.5°$): (a) on the graphene coated part, (b) without the graphene buffer layer; XRD pole figures for the GaN $\{0002\}$ ($2\theta = 34.6°$): (c) on the graphene coated part, (d) without the graphene buffer layer. $\Psi = 0°–75°$, $\varphi = 0–360°$.

for the parts of the same wafer without multilayer graphene buffer which clearly indicates growth of polycrystalline GaN film.

SEM images of the GaN film grown on graphene/SiO_2 substrate [Fig. 3(a)] demonstrate a smooth surface morphology with relatively low density of structural defects. The $2\theta/\omega$ XRD scan [Fig. 4(a)] of the GaN film grown on amorphous SiO_2 substrates with graphene buffer layer shows eight peaks at $2\theta = 26.5°$, 32.98°, 34.62°, 36.0°, 69.1°, 72.95°, 76.4°, 116.6° and 126.2°, which can be attributed to the diffractions from multilayer graphene,[8,10] Si (200)[24] GaN (0002),[25] AlN (0002),[26] Si (400),[27] GaN (0004),[25] AlN (0004),[26] Si (600) and GaN (0006)[25] planes, respectively. The full width at half maximum (FWHM) of the (0002) rocking curve of GaN on multilayer graphene buffer was 12 arcmin. This value agrees well with the literature data[11] for PA-MBE on 1 ML graphene coated monocrystalline silicon without amorphous SiO_2 insert (11.3 arcmin) and it is noticeably lower than those for GaN obtained by MOCVD on ZnO/graphene coated SiO_2 (48 arcmin)[8] or obtained by PA-MBE on the surface of graphene coated copper foil (17.2 arcmin)[15]. The $\{10\bar{1}3\}$ XRD pole figure [Fig. 5(a)] demonstrates a six-fold rotational symmetry, which is typical for hexagonal GaN crystal, while Fig. 5(c) indicates the good *c*-axis orientation of the GaN film.

Simultaneously, SEM image analysis shows that the GaN film grown without the graphene buffer layer [Fig. 3(b)] has polycrystalline fine-grained (200–300 nm) morphology. The X-ray diffraction spectrum obtained from these regions of the wafer [Fig. 4(b)] contains, in addition to the above listed, two more peaks at $2\theta = 63.5°$ and 105.1° (diffractions from $(10\bar{1}3)$[25] and $(10\bar{1}5)$[25] GaN planes). Moreover, the second (0004) and third (0006) order diffraction lines from the GaN (0002) base planes have a low intensity. In turn, the GaN film grown on amorphous SiO_2 substrate showed a broad ring-shaped pattern in the $\{10\bar{1}3\}$ XRD pole figure [Fig. 5(b)] and a broad spot in the center of $\{0002\}$ XRD pole figure [Fig. 5(d)], which indicates the formation of polycrystalline

© 2019 The Japan Society of Applied Physics

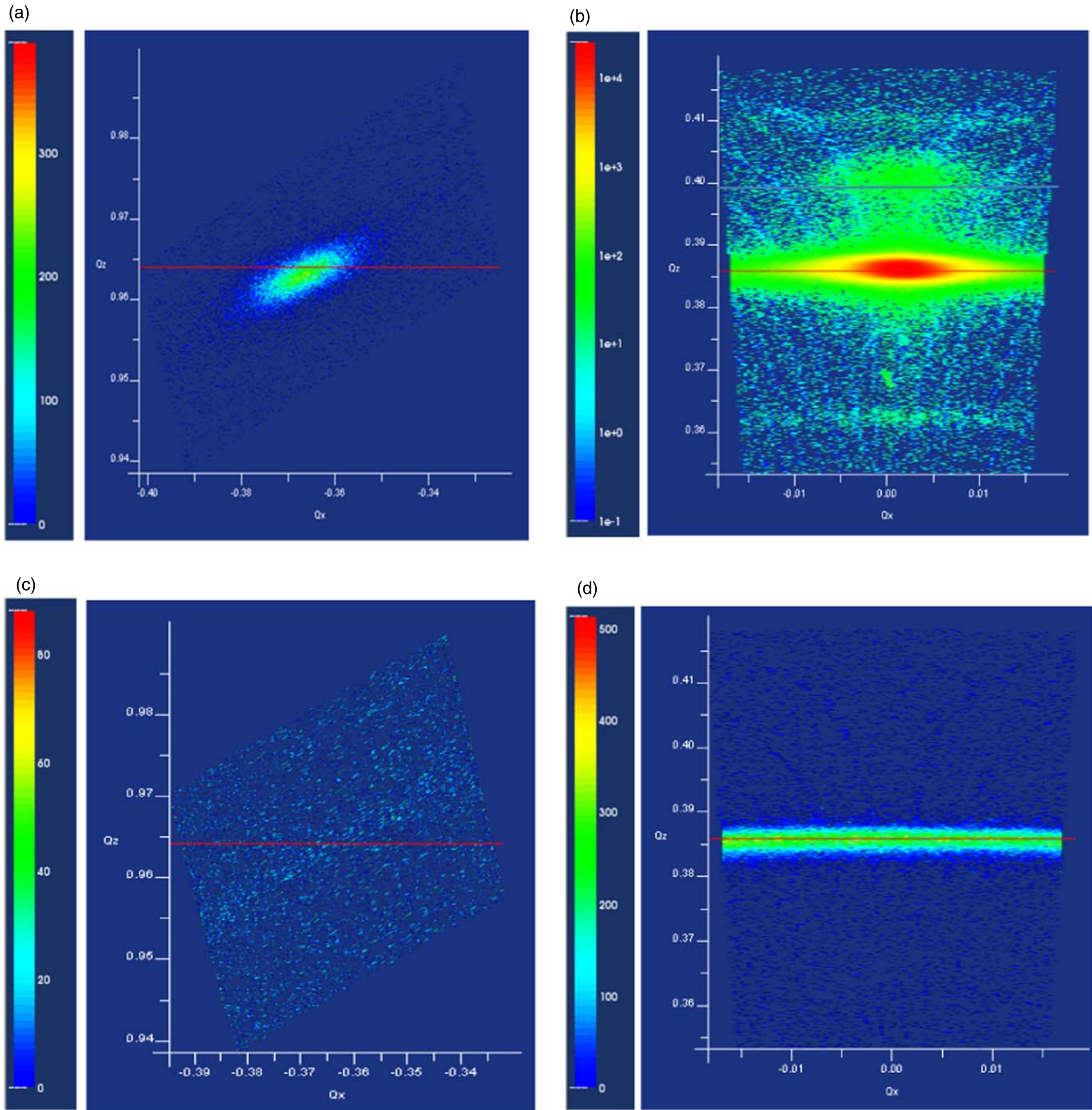

Fig. 6. (Color online) RSM data: around GaN $10\bar{1}5$ reflection (asymmetric) from the graphene coated part of the wafer (a); around GaN 0002 reflection (symmetric) from graphene coated part of the wafer (b); around GaN $10\bar{1}5$ reflection (c) and 0002 reflection (d) from the part of the same wafer without the graphene buffer layer. Reciprocal coordinates are shown in $Å^{-1}$(1/d)).

film with weak texture along the growth direction and is consistent with the fine-grained surface morphology observed by the SEM method.

The measurements of reciprocal space maps (RMS) of symmetric 0002 and asymmetric $10\bar{1}5$ GaN reflections were carried out to determine the lattice parameters of GaN epilayer and to estimate the strain relaxation. Figure 6(a) demonstrates the RSM around $10\bar{1}5$ GaN reflection from graphene coated part of the wafer. As we can see from Fig. 6(a) the interplanar spacing d_{0002} calculated using RSM date ($d_{0002} = (\frac{2}{5}\Delta Q_z)^{-1}$) is 2.595 Å, which is close to tabular value 2.593 Å for GaN[25] (red line). Also, the peak position on the asymmetrical $10\bar{1}5$ GaN RSM indicates that the $(10\bar{1}0)$ interplanar spacing ($d_{10.0} = (\Delta Q_x)^{-1}$) is equal to 2.74 Å. Comparing this value with tabular data for interplanar distance $d_{10.0}(\sqrt{3}\,a_{GaN}/2) = 2.762$ Å in GaN and for graphene lattice parameter $a_{gr} = 2.46$ Å[28] will lead to a strain relaxation R of about 93% at expected lattice mismatch parameter of 12.2%. With the lattice parameters derived above, the in-plane and out-of-plane strain in the GaN layer can be then calculated from equations:[29,30]

$$\varepsilon_a = \frac{d_{10.0} - d_{10.0}^{ref}}{d_{10.0}^{ref}} \text{ and } \varepsilon_c = \frac{d_{0002} - d_{0002}^{ref}}{d_{0002}^{ref}}$$

where index "*ref*" denotes the unstrained layer. The calculated strains are -8×10^{-3} and $+7.7 \times 10^{-4}$. These values are in good agreement with the literature data[28,29] for MBE

© 2019 The Japan Society of Applied Physics

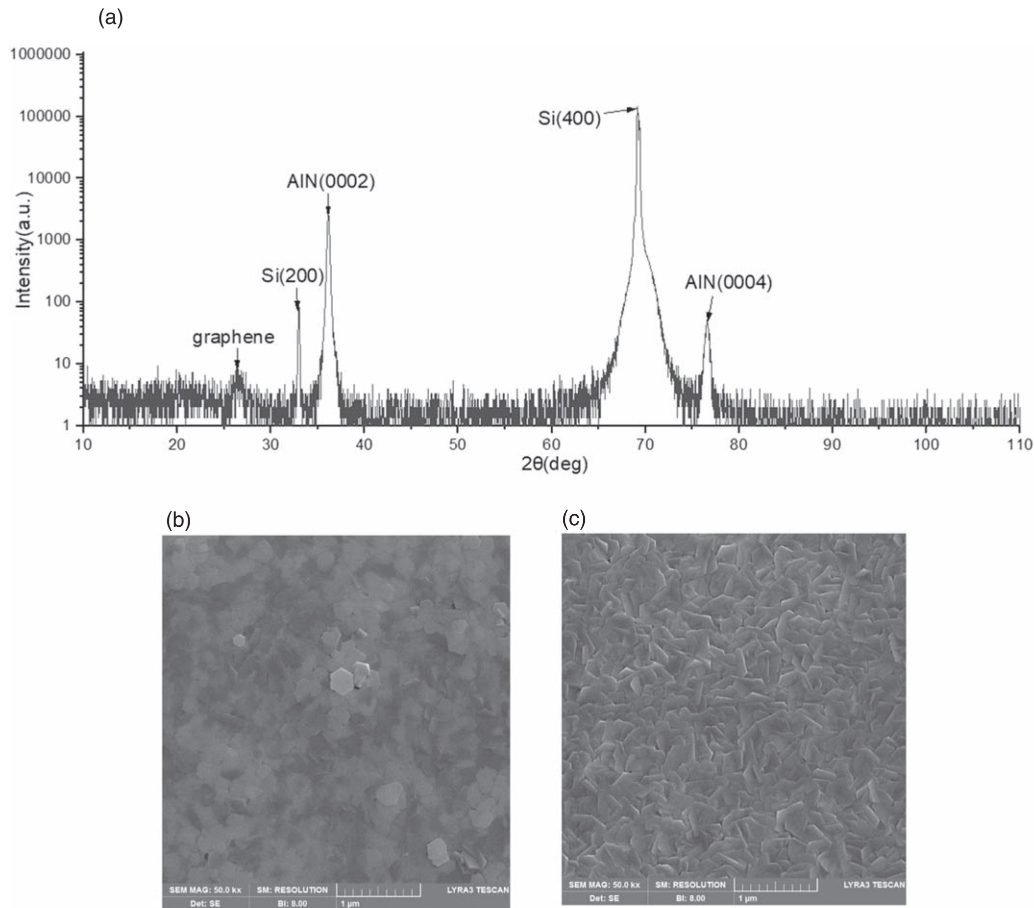

Fig. 7. XRD spectrum of AlN film grown on multilayer graphene buffer (a). SEM images: (b)–the surface of AlN film on graphene coated part of the wafer, (c)–the surface of AlN film deposited directly on SiO_2.

grown GaN films on Al_2O_3. However, some of the GaN domains turn up by an angle of 30° around the growth axis (*c*) relative to the above specified position, as it follows from Fig. 5(a). Obviously, the content ratio of such domains in the layer can be appreciated from their lines intensities ratio on azimuthal φ section of $\{10\bar{1}3\}$ GaN pole figure. In our case, this ratio is about 0.11 (11%).

In turn Fig. 6(b) demonstrates the RSM around GaN 0002 reflection from graphene coated part. There are two clear spots here corresponding to the reflection from the GaN (0002) (marked with a red line) and AlN (0002) planes (marked with a blue line). The intensity of reflection in the latter case is lower due to the low thickness of AlN nucleation layer. At the same time, the RSM from the part of the wafer without graphene buffer shows that the GaN crystallites are highly disoriented [Figs. 6(c), 6(d)], i.e. there is a polycrystal.

Similar results were obtained for AlN layers. The XRD scan [Fig. 7(a)] of 300 nm thick AlN film grown on SiO_2 substrates with graphene buffer shows five peaks at $2\theta = 26.5°$, 32.98°, 36.1°, 69.1° and 76.6°, which can be attributed to the diffractions from multilayer graphene,[8,10] Si (200),[24] AlN (0002),[26] Si (400),[27] and AlN (0004)[26] planes, respectively. While the FWHM of the (0002) AlN rocking curve is 14.4 arcmin. In contrast to the graphene coated part, the XRD spectrum of AlN film on SiO_2 (not shown here) contains two additional peaks at 50.2° and 95.2° which corresponds to the diffraction from $(20\bar{2}3)$[26] and $(10\bar{1}2)$[26] atomic planes. SEM images of respective parts of the wafer are shown in Figs. 7(b), 7(c).

4. Conclusions

In this paper, the possibility of CVD graphene using as a 2D buffer layer for epitaxial growth of III-nitrides by PA-MBE on amorphous substrates was investigated. The multilayer graphene films were grown by the CVD method on 60 μm thick copper foil using n-decane ($C_{10}H_{22}$) as a carbon source and then transferred onto the surface of 2-inch Si wafers with 300 nm thick thermal oxide. Graphene film thickness according to optical and micro-Raman measurement[16,17] was 2–3 monolayers. After that GaN and AlN epilayers were grown by PA-MBE under the metal-rich conditions using the HT AlN nucleation layer. The comparative study of graphene-coated parts of the wafers and the parts without graphene was carried out by SEM and HRXRD including XRD pole figures method. The nucleation and growth was also monitored in situ by RHEED technique. It was shown that epitaxial GaN and AlN films with Me polarity and close to 2D surface morphology can be obtained by PA-MBE on amorphous SiO_2 substrates with multilayer graphene buffer. The FWHM of the (0002) rocking curve of GaN on multilayer graphene was 12 arcmin. This value agrees well with the literature data[11] with significant gain in surface morphology. Similar results were obtained for AlN layers (14.4 arcmin).

The key problem confronted in this study is difficult in experimentallt determining the relative orientation of $A^{III}N$

© 2019 The Japan Society of Applied Physics

and graphene film in view of the fact that the graphene layers lie freely on the surface of the silicon oxide and do not have any epitaxial relationships with the Si wafer. This problem will be solved in the framework of future research.

Acknowledgments

This work was carried out using the equipment of MEPhI Shared-Use Equipment Center ≪Heterostructural Microwave Electronics and Wide Band Gap Semiconductor Physics≫ (http://ckp-nano.mephi.ru).

ORCID iDs

D. P. Borisenko https://orcid.org/0000-0002-3249-9630

1) I. Akasaki, Rev. Mod. Phys. **87**, 1119 (2015).
2) S. Nakamura et al., Appl. Phys. Lett. **69**, 4056 (1996).
3) V. Kumar et al., Solid-State Electron. **47**, 1577 (2003).
4) M. Khan et al., Appl. Phys. Lett. **63**, 1214 (1993).
5) A. Dadgar et al., J. Cryst. Growth **248**, 556 (2003).
6) H. Morkoç"General properties of nitrides," *In Handbook of Nitride Semiconductors and Devices*, ed. H. Morkoç (Wiley-VCH, Weinheim, 2009).
7) K. Chung et al., Science **330**, 655 (2010).
8) K. Chung et al., NPG Asia Mater. **4**, e24 (2012).
9) H. Yoo, K. Chung, Y. S. Choi, C. S. Kang, K. H. Oh, M. Kim, and G.-C. Yi, Adv. Mater. **24**, 515 (2012).
10) J. W. Shon et al., Sci. Rep. **4**, 5325 (2014).
11) T. Araki et al., Applied Physics Express **7**, 071001 (2014).
12) T. H. Seo et al., Sci. Rep. **5**, 7747 (2015).
13) T. Li et al., AIP Adv. **8**, 045105 (2018).
14) Z. Chen et al., Adv. Mater. **30**, 1801608 (2018).
15) J. Yu et al., Alloys and Compounds **783**, 633 (2019).
16) I. V. Komissarov et al., Beilstein J. Nanotechnol. **8**, 145 (2017).
17) M. S. Tivanov et al., Journal of Applied Spectroscopy **84**, 6 (2018).
18) D. V. Nechaev et al., J. Cryst. Growth **425**, 9 (2015).
19) V. N. Jmerik et al., J. Cryst. Growth **354**, 9 (2012).
20) Z. Lu et al., ACS Appl. Mater. Interfaces **9**, 23081 (2017).
21) Y. Tchoe et al., NPG Asia Mater. **7**, e206 (2015).
22) S. Hasegawa,"Reflection high-energy electron diffraction," *Characterization of Materials*, ed. E. N. Kaufmann (Wiley, New York, 2012).
23) A. R. Smith et al., Appl. Phys. Lett. **72**, 2114 (1998).
24) P. Zaumseil, J. Appl. Cryst. **48**, 528 (2015).
25) ICDD: 00-050-0792.
26) ICDD: 00-025-1133.
27) ICDD: 00-005-0565.
28) J. Warner et al., *Graphene. Fundamentals and Emergent Applications* (Elsevier Oxford, 2013).
29) V. S. Harutyunyan et al., J. Phys. D: Appl. Phys. **34** (2001)A35.
30) M. K. Mahata et al., AIP Adv. **4**, 117120 (2014).

© 2019 The Japan Society of Applied Physics